Electrostatic Environment of the Tryptophylquinone Cofactor in Methylamine Dehydrogenase: Evidence from Resonance Raman Spectroscopy of Model Compounds†

Pierre Moënne-Loccoz,‡ Nobuhumi Nakamura,‡ Shinobu Itoh,§ Shunichi Fukuzumi,§ Antonius C. F. Gorren,|| Johannis A. Duine,|| and Joann Sanders-Loehr*,‡

Department of Chemistry, Biochemistry, and Molecular Biology, Oregon Graduate Institute of Science and Technology, Portland, Oregon 97291-1000, Department of Applied Chemistry, Faculty of Engineering, Osaka University, 2-1 Yamada-oka, Suita, Osaka 565, Japan, and Department of Microbiology and Enzymology, Delft University of Technology, 2628 BC Delft, The Netherlands

Received November 6, 1995; Revised Manuscript Received January 23, 1996⊗

ABSTRACT: Methylamine dehydrogenase (MADH) utilizes its endogenous tryptophan tryptophylquinone (TTQ) as a cofactor in enzymatic catalysis, with the C6 carbonyl of the quinone implicated as the site of attack by substrates and other nucleophiles. Resonance Raman (RR) spectroscopy provides an ideal method for investigating the state of this carbonyl group whose C═O stretch is distinct from other vibrational modes of the cofactor and is readily identified by its shift to lower energy in $H_2{}^{18}O$. In a series of indole 6,7-quinone models for TTQ, the in-phase stretching vibration of the two C═O groups occurs at 1650 cm^{-1} in nonpolar solvents and shifts to 1638 cm^{-1} in H_2O. The absorption maximum undergoes an analogous shift from 400 to 425 nm. The spectral properties of the indole quinones in H_2O approach the corresponding values in *Thiobacillus versutus* MADH (C═O stretch at 1612 cm^{-1}, λ_{max} at 440 nm) and are indicative of strong hydrogen bonding of the C═O and NH groups of the cofactor in the native enzyme. Addition of monovalent cations [NH_4^+, Cs^+, and $(CH_3)_3NH^+$] to MADH causes further increases in the λ_{max} and decreases in the frequency of the C═O stretch [1590 cm^{-1} with $(CH_3)_3NH^+$]. This implies a strong electrostatic interaction between monovalent cations and a carbonyl oxygen (most likely at C6) in TTQ. The fact that these cations behave as competitive inhibitors of the methylamine substrate suggests that methylamine binds to the same location in the enzyme prior to its covalent reaction with the cofactor. Addition of monovalent cations to the one-electron-reduced semiquinone form of MADH results in RR spectral shifts for a number of vibrational modes of the cofactor. Thus, the ability of monovalent cations to promote and stabilize the formation of the semiquinone intermediate is also due to their direct electrostatic interaction with the TTQ cofactor.

Methylamine dehydrogenase (MADH, EC 1.4.99.3) carries out the oxidation of methylamine to formaldehyde, allowing certain methylotrophic bacteria to grow on methylamine as their sole carbon and energy source (Davidson, 1993; Duine, 1993). This reaction is catalyzed by a covalently bound tryptophan tryptophylquinone cofactor (TTQ, Figure 1) whose structure has been verified by DNA sequencing, NMR spectroscopy, and X-ray crystallography (McIntire et al., 1991a; Chen et al., 1991). The two-electron oxidation of the substrate is accompanied by transamination, yielding the reduced aminophenol form of the TTQ cofactor. The quinone form, $MADH_{ox}$, is regenerated by two consecutive electron transfers to amicyanin, passing through a semiquinone intermediate, $MADH_{SQ}$ (Backes et al., 1991).

The X-ray structure of the electron-transfer complex of $MADH_{ox}$ and amicyanin from *Paracoccus denitrificans* shows the tryptophyl ring of the TTQ cofactor to be close to the subunit interface and only 9.3 Å from the electron-accepting Cu site in amicyanin (Chen et al., 1992). The quinone moiety of the tryptophylquinone ring is buried within the small subunit of MADH, having its NH and C7 carbonyl groups hydrogen-bonded to the polypeptide backbone and its C6 carbonyl more accessible (Chen et al., 1991). The assignment of the C6 carbonyl as the site of nucleophilic attack by substrate is supported by crystal structures of *Thiobacillus versutus* MADH which show that hydrazines add to the C6 position of the cofactor (Huizinga et al., 1992). In addition, there is an immobilized solvent molecule interacting with the C6 carbonyl oxygen (Figure 1) that was originally ascribed as either an ammonium ion or a water molecule (Huizinga et al., 1992). More recent studies have shown that cations such as NH_4^+, Cs^+, and $(CH_3)_3NH^+$, which serve as competitive inhibitors of substrate binding, also cause significant shifts in the absorption spectrum of the TTQ cofactor (Gorren & Duine, 1994; Kuusk & McIntire, 1994). These studies suggest that there is a cation binding site in close proximity to the quinone group.

† This research was supported by the grants from the U.S. Public Health Service, National Institutes of Health GM-34468 and National Science Foundation BIR-9216592 (J.S.-L.), Grant-in-Aid for Scientific Research from the Ministry of Education, Science, and Culture of Japan (S.I. and S.F.), and the Dutch Organization for Scientific Research (J.A.D.).

* Author to whom correspondence should be addressed at Department of Chemistry, Biochemistry and Molecular Biology, Oregon Graduate Institute of Science and Technology, Portland, OR 97291-1000. Phone: 503-690-1079. Fax: 503-690-1464.

‡ Oregon Graduate Institute of Science and Technology.

§ Osaka University.

|| Delft University of Technology.

⊗ Abstract published in *Advance ACS Abstracts,* April 1, 1996.

0006-2960/96/0435-4713$12.00/0

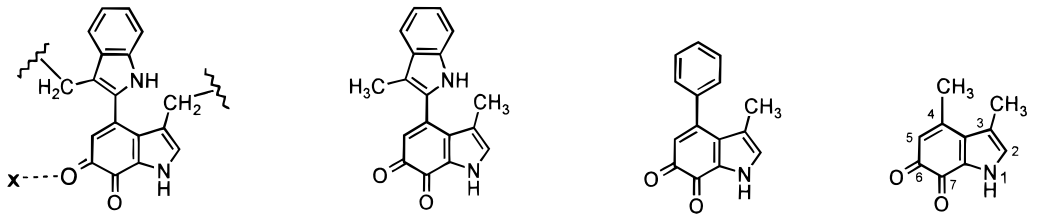

FIGURE 1: Structure of tryptophan tryptophylquinone cofactor of MADH (6,7-TTQ) and indole quinone model compounds with indole (6,7-IIQ), phenyl (6,7-PIQ), and methyl (6,7-MIQ) groups in place of the tryptophyl ring of TTQ. X = the location of an NH_4^+ ion in the X-ray structure of *T. versutus* MADH (Huizinga et al., 1992).

Raman spectroscopy, a light-scattering technique which measures molecular vibrations, also provides valuable structural details about protein active sites (Carey, 1982). Excitation within the visible absorption band of quinones leads to a resonance Raman (RR) spectrum with numerous peaks between 1000 and 1700 cm^{-1} that are primarily due to C═C, C═O, C═N, and C−H vibrations of the quinone ring (Dooley & Brown, 1993). Although vibrational assignments are complicated by the fact that these motions tend to be strongly coupled with one another, we have found that the C═O in-phase stretch of the quinone is a fairly pure mode for both the TTQ cofactor in MADH (Backes et al., 1991) and the trihydroxyphenylalanine quinone of amine oxidases (Moënne-Loccoz et al., 1995). In $MADH_{ox}$, the C═O stretch occurs at ∼1620 cm^{-1} and is identified by its downshift of ∼22 cm^{-1} upon incubation in $H_2{}^{18}O$ (McIntire et al., 1991b; Backes et al., 1991). The unusually low C═O stretching frequency in MADH compared to the more typical quinone value of ∼1675 cm^{-1} (Singh & Singh, 1968; Nonaka et al., 1990) has been ascribed to hydrogen bonding of the carbonyl oxygen in the protein (Backes et al., 1991). In addition, the C═O stretch in MADH was found to shift another 5−30 cm^{-1} to lower energy in the presence of cations such as NH_4^+, Cs^+, and $(CH_3)_3NH^+$ (Gorren et al., 1995a). The specificity of this reaction has now been verified by showing that the C═O stretch has the greatest sensitivity to $H_2{}^{18}O$ as well as cations. Although such a cation binding site has been suggested by other techniques, X-ray crystallography cannot identify the chemical species bound as an exogenous ion, and absorption spectroscopy cannot identify what part of the cofactor it is interacting with. Our RR data provide the first direct evidence that these cations occupy a binding site adjacent to a carbonyl oxygen of the TTQ cofactor.

Recently, an indole quinone model compound (6,7-IIQ, Figure 1) has been synthesized that is an excellent model for the TTQ cofactor in MADH (Itoh et al., 1992, 1995). It mirrors the enzyme in its electronic and RR spectral properties as well as in its ability to catalyze the oxidation of benzylamine (Itoh et al., 1995; Ohshiro & Itoh, 1994). The C6 carbonyl group appears to be the preferred position for nucleophilic addition in 6,7-IIQ as well as in the native enzyme. Two other indole quinone model compounds with phenyl (6,7-PIQ) and methyl (6,7-MIQ) substituents (Figure 1) have also been synthesized. We have found that the RR spectra of these model compounds have similar ^{18}O- and D-isotope dependence to *T. versutus* MADH, thereby verifying our spectral assignments. Furthermore, the electronic and RR spectral properties of these model compounds, particularly the C═O stretch, are strongly dependent on the polarity of the solvent, thereby allowing us to draw firmer conclusions about the electrostatic environment of the TTQ cofactor in MADH.

EXPERIMENTAL PROCEDURES

Synthesis of Model Compounds. The 3-methyl-4-(3′-methylindol-2′-yl)indole-6,7-dione (6,7-IIQ), 3-methyl-4-phenylindole-6,7-dione (6,7-PIQ), and 3,4-dimethylindole-6,7-dione (6,7-MIQ), whose structures are shown in Figure 1, were obtained from previous studies[1] (Ohshiro & Itoh, 1994; Itoh et al., 1995). Isotope exchange with $H_2{}^{18}O$ (97 atom %, ICON) or D_2O (99 atom %, Merck) was achieved by dissolving the model compound in CH_3CN and adding 1−3 volumes of the desired water isotope for RR spectroscopy and 0.13 volume for mass spectrometry. Complete isotope incorporation was obtained within 15 min at room temperature.

MADH Samples. MADH from *T. versutus* was purified as described previously (van Wielink et al., 1990) and stored frozen as a concentrated solution (0.26 mM) in 100 mM acetate (pH 5.0). For Raman experiments, samples were diluted into the desired buffer and reconcentrated to 0.2 mM with a Microcon 30 (Amicon) ultrafiltration device. The ^{18}O-labeled $MADH_{ox}$ prepared by 10-fold dilution into bicine buffer (pH 9.0) in $H_2{}^{18}O$ (97 atom %, ICON) and a 12 h incubation, followed by reconcentration to yield a sample 87 atom % in $H_2{}^{18}O$. The completeness of exchange was monitored by RR spectroscopy which showed no further downshifts of the 1612-cm^{-1} C═O stretch with longer incubation times.

The semiquinone was prepared from concentrated $MADH_{ox}$ (0.26 mM) in 25 mM bicine buffer (pH 9.0) in an argon-flushed capillary and used directly for optical and RR experiments. The one-electron reduction of MADH by dithionite, which was monitored spectroscopically to yield the maximum concentration of SQ and minimum concentration of quinone, required ∼1.5 equiv of dithionite per TTQ (in part due to residual O_2 in the system). Concentrated anaerobic solutions of cations were added to $MADH_{SQ}$ after the completion of this titration. The ^{18}O-labeled SQ was prepared by the addition of dithionite to ^{18}O-labeled $MADH_{ox}$, yielding a sample 80 atom % in $H_2{}^{18}O$ and ∼0.2 mM in protein.

Spectroscopy. Raman spectra were obtained on a custom McPherson 2061/207 spectrograph (0.67-m focal length, 1800-groove grating, 8-cm^{-1} spectral resolution) using Kaiser Optical holographic super-notch filters and a Princeton

[1] Details of the synthetic procedures for 6,7-PIQ and 6,7-MIQ will be reported elsewhere.

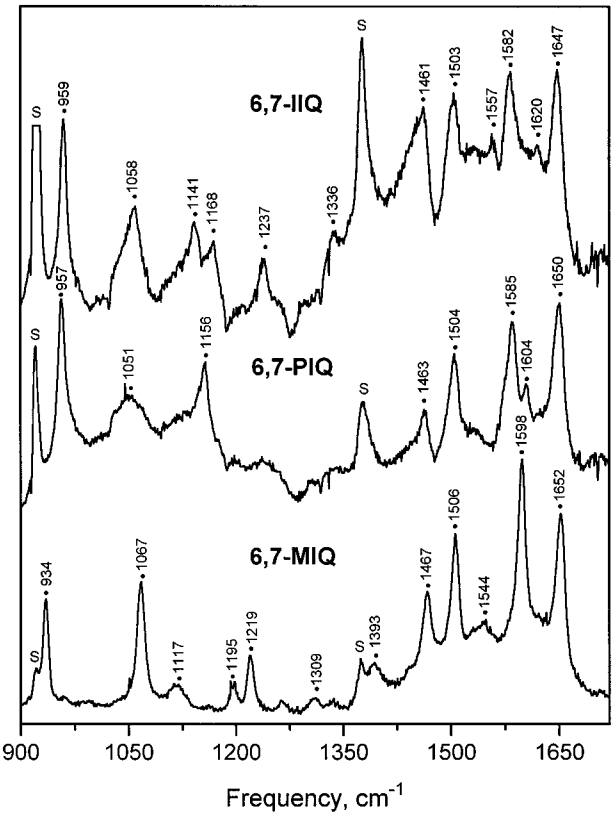

FIGURE 2: Resonance Raman spectra of 6,7-IIQ, 6,7-PIQ, and 6,7-MIQ at a concentration of $\sim 5 \times 10^{-4}$ M in acetonitrile. Spectra obtained at room temperature with 413-nm excitation (20 mW). "S" indicates Raman bands from acetonitrile solvent.

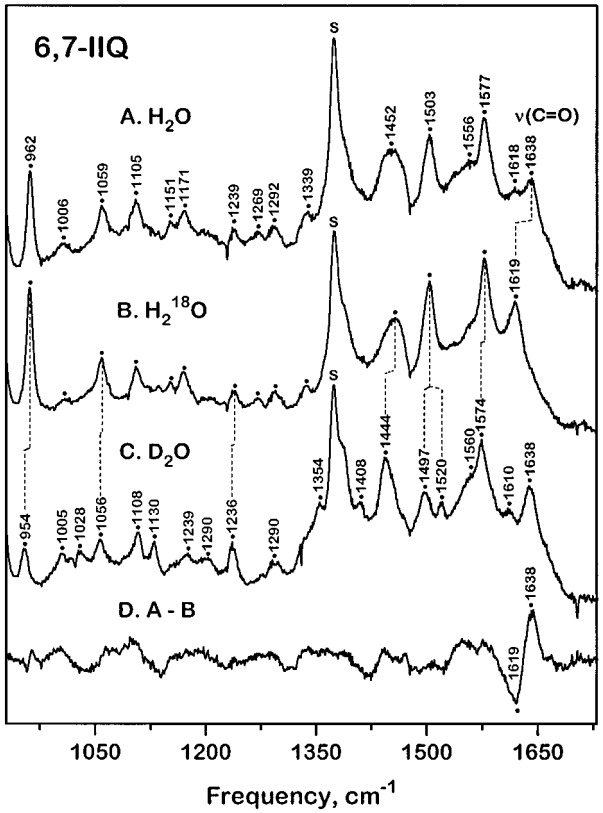

FIGURE 3: Resonance Raman spectra of 6,7-IIQ in (A) $H_2{}^{16}O$, (B) $H_2{}^{18}O$, and (C) D_2O. Spectrum D is a difference spectrum for the sample in $H_2{}^{16}O$ minus the sample in $H_2{}^{18}O$. The sample was dissolved in a 1:1 mixture of water and acetonitrile and spectra were obtained as in Figure 2. Marked peaks in panel B have the same frequencies as in panel A.

Instruments (LN-1100PB) liquid-N_2-cooled CCD detector. Excitation sources were provided by Liconix 4240PS He-Cd (442 nm), Coherent Innova 90 Ar (488 nm), and Innova 302 Kr (413 nm) lasers. Spectra were collected using a 90°-scattering geometry and a 5-min accumulation time on samples in glass capillaries at room temperature or inserted into a cold finger immersed in a water−ice mixture for cooling to 278 K (Loehr & Sanders-Loehr, 1993). Peak frequencies were calibrated relative to an indene standard and are accurate to ± 1 cm^{-1}. Spectra of samples substituted with isotopes or cations were obtained under identical instrumental conditions such that frequency shifts are accurate to ± 0.5 cm^{-1}. In cases where peaks are overlapping, reported peak frequencies are based on curve resolving. Mass spectra were recorded with a JEOL JNX-DX303 HF mass spectrometer in the electron-impact mode.

RESULTS AND DISCUSSION

Resonance Raman Spectra of Indole Quinones. RR spectra of 6,7-IIQ, 6,7-PIQ, and 6,7-MIQ with 4-indolyl, phenyl, and methyl substituents, respectively (Figure 1) have been obtained for samples in acetonitrile (Figure 2). The spectra of these three compounds are strikingly similar, particularly in the 1450−1700 cm^{-1} region which is dominated by C═C and C═O stretching modes. Each compound exhibits a set of four intense bands at ~1465, 1505, 1585, and 1650 cm^{-1}. All of these peaks show upshifts of 2 cm^{-1} or more on going from 6,7-IIQ to 6,7-PIQ and 6,7-MIQ that are probably due to the inductive effect of the substituent at the 4-position of the indole quinone. However, the overall similarity of the RR spectra indicates that the vibrational motions of the 4-indolyl, phenyl, and methyl substituents are not part of the indole quinone chromophore. The lack of conjugation between the two π systems in 6,7-IIQ and 6,7-PIQ is most likely due to a non-coplanar arrangement of the two aromatic rings. These results are consistent with the calculated dihedral angle of 46.9° for the two indole rings in 6,7-IIQ (Itoh et al., 1995).

When 6,7-IIQ is placed in a more polar environment by addition of an equal volume of water to the acetonitrile solution, three of the dominant peaks shift by −9, −5, and −9 cm^{-1}, respectively, to 1452, 1577, and 1638 cm^{-1} (Figure 3). Similar shifts are observed for MIQ in a 3:1 mixture of H_2O and acetonitrile, with the greatest shift of −13 cm^{-1} occurring for the 1639-cm^{-1} mode (Table 1). These downshifts are most likely due to electrostatic effects arising from hydrogen bonding. The RR spectra of the indole quinone models in aqueous media are particularly close to $MADH_{ox}$, which exhibits intense vibrational modes at ~1450, 1565, and 1620 cm^{-1} (Table 1). The similarity of the spectra indicate that, as with the model compounds, only the quinone ring of the TTQ cofactor contributes to the RR spectrum. The lack of conjugation is in agreement with the 42° dihedral angle between the two indole rings in the X-ray crystal structure of $MADH_{ox}$ (Chen et al., 1991).

^{18}O-Isotope Shifts. To place the frequency correlations between the tryptophylquinone of MADH and the indole quinones of the model compounds on a firmer footing, we investigated the effects of ^{18}O-carbonyl exchange on the RR spectrum of 6,7-IIQ. Incubation of 6,7-IIQ in $H_2{}^{18}O$ results in a 19 cm^{-1} downshift of the 1638 cm^{-1} mode (Figure 3B). The frequency and mass dependence of this mode allows it to be assigned to the in-phase stretch of the two C═O groups.

Table 1: Raman Frequencies of Quinones in MADH and Model Compounds[a]

tryptophylquinone in MADH									indole quinone in model compounds						
T. versutus[b]			*P. denitrificans*[c]			*M.* strain W3A1[d]			6,7-IIQ[e]				6,7-MIQ[f]		
ν	$[\Delta^{18}O]$	$\{\Delta N^+\}$	ν	$[\Delta^{18}O]$	$\{\Delta N^+\}$	ν	$[\Delta^{18}O]$	(ΔD)	ν	$[\Delta^{18}O]$	(ΔD)	$\{\Delta aq\}$	ν	$[\Delta^{18}O]$	$\{\Delta aq\}$
1612	[−19]	{−22}	**1625**	[−16]	{−26}	**1614**	[−27]	(−3)	**1638**	[−19]		{−9}	1639	[−27]	{−13}
1563		{−11}	**1570**	[−18]	{−11}	**1558**		(−2)	**1577**		(−3)	{−5}	**1596**	[−3]	{−2}
1528		{−6}	1531		{−4}	1518		(−14)					1542	[−5]	{−2}
1487		{−2}	1490		{−2}	1481			**1503**		(−6)		**1509**	[−2]	{+3}
1452		{−3}	**1454**		{−4}	**1448**		(−6)	**1452**		(−8)	{−9}			

[a] Frequencies in cm^{-1}. Boldface denotes most intense peaks. Frequency shifts in $H_2{}^{18}O$ and D_2O denoted by $[\Delta^{18}O]$ and (ΔD), respectively. $\{\Delta N^+\}$ refers to frequency shift in the presence of 10 mM $(CH_3)_3NH^+$. $\{\Delta aq\}$ refers to frequency in aqueous solvent relative to pure acetonitrile. [b] Spectra obtained as in Figure 6. [c] Spectra at 15 K from Backes et al. (1991) except $(CH_3)_3NH^+$ data obtained as in Figure 6 with enzyme provided by Dr. V. L. Davidson. [d] *Methylophilus sp.* strain W3A1. Spectra at 298 K from McIntire et al. (1991b). [e] Spectra obtained as in Figure 2 on samples dissolved in water/acetonitrile (1:1). [f] Spectra obtained as in Figure 2 on samples dissolved in water/acetonitrile (3:1).

The difference spectrum for $H_2{}^{16}O$ minus $H_2{}^{18}O$ reveals a lack of ^{18}O-dependent shifts in any of the other peaks (Figure 3D), thereby indicating that the C═O stretch is a fairly pure mode and not coupled to other vibrations. In such a case, substitution of both carbonyl oxygens of 6,7-IIQ would be expected to result in a 40 cm^{-1} downshift. The fact that a shift of only 19 cm^{-1} is observed indicates that only one C═O has exchanged with solvent. This was verified by mass spectrometry where 6,7-IIQ in $H_2{}^{18}O$ yielded new peaks at m/z 292 (M^+) and 294 (M^++2, characteristic of *o*-quinones) compared to peaks at 290 and 292, respectively in $H_2{}^{16}O$. Since nucleophiles such as cyclopropylamine and benzylamine both react preferentially with the C6 carbonyl of 6,7-IIQ (Ohshiro & Itoh, 1994), it is likely that C6 is also the site of adduct formation with water. In this mechanism, [^{18}O]-hydroxide adds to the quinone ring to produce a dihydroxo intermediate containing ^{16}OH and ^{18}OH at C6, and the subsequent loss of [^{16}O]hydroxide and H^+ yields the C═^{18}O product at C6. Furthermore, our observation that 6,7-IIQ derivatized at the C6 position with dinitrophenylhydrazine shows no ^{18}O-dependence in its RR spectrum lends further support to our conclusion that only the C6 carbonyl reacts with water.

The X-ray structure of *T. versutus* MADH has shown that hydrazines selectively add to the C6 carbonyl (Huizinga et al., 1992), thereby revealing that the C6 position is the preferred site of nucleophilic attack in the enzyme as well as in the 6,7-IIQ model. The occurrence of a C═O stretching mode at 1638 cm^{-1} in 6,7-IIQ and 1639 cm^{-1} in 6,7-MIQ (Table 1) is also similar to the vibrational behavior of TTQ. MADHs from three different organisms exhibit an analogous C═O stretch at 1612−1625 cm^{-1} that downshifts by 16−27 cm^{-1} upon ^{18}O-substitution (Table 1). The ^{18}O-dependence of the protein spectra is similarly indicative of exchange of only a single carbonyl oxygen, most likely at the C6 position. The C═O vibration in *T. versutus* MADH (Figure 6) is not as distinct as in the other two MADH enzymes (Table 1) or in the indole quinone models (Figures 2 and 3). Nevertheless, the difference spectrum in Figure 6C provides clear evidence for an isotope shift for the peak at ∼1616 cm^{-1} and no other isotope dependence anywhere else in the spectrum. Curve-resolving places the C═O stretch at 1612 cm^{-1} in $H_2{}^{16}O$ and 1593 cm^{-1} in $H_2{}^{18}O$ in *T. versutus* MADH (Table 1).

The actual frequency of the C═O stretch, ν(C═O), is sensitive to the nature of the quinone as well as to its electrostatic environment. The indole quinones in nonpolar solvents have ν(C═O) values of 1647−1652 cm^{-1} (Figure 2), which are 20−30 cm^{-1} lower than the values of 1666−1681 cm^{-1} for TPQ (trihydroxyphenylalanine quinone) in amine oxidase and model compounds (Moënne-Loccoz et al., 1995) and 1675 cm^{-1} for the *p*-quinones, 1,4-naphthoquinone and 9,10-anthraquinone (Singh & Singh, 1968; Nonaka et al., 1990). This difference appears to be due mainly to the *o*-quinone character of the 6,7-IIQ compounds since the *o*-quinone, 4,5-IQ, has a similarly low ν(C═O) of 1655 cm^{-1} whereas the *p*-quinone, 4,7-IQ has its ν(C═O) at 1667 cm^{-1} (J. Sanders-Loehr, N. Nakamura, and S. Itoh, unpublished results). Increasing the polarity of the environment by addition of H_2O causes ν(C═O) of the indole quinone models to drop to 1638−1639 cm^{-1} (Table 1), which is still 13−24 cm^{-1} higher than the value in the proteins. This indicates that the carbonyl oxygens may be more strongly hydrogen bonded inside the protein. Interestingly, 6,7-IIQ in the solid state (where it can undergo intermolecular hydrogen bonding) has its ν(C═O) at 1620 cm^{-1} (Itoh et al., 1995), which is within the protein range.

D-Isotope Shifts. Shifts in vibrational frequencies in D_2O can be due to mass effects from the exchange of ring protons or to electrostatic effects arising from different hydrogen bond strengths for H versus D. Mass effects can cause shifts of 10−20 cm^{-1} due to coupling of the NH bend, δ(N−H), with ring stretching modes, whereas shifts due to H-bonding effects are generally <5 cm^{-1}. Incubation of 6,7-IIQ with D_2O causes downshifts of 3−8 cm^{-1} in at least six different vibrational modes (Figure 3C and Table 1). These profound changes in the RR spectrum of 6,7-IIQ, which are reminiscent of D-isotope effects on the RR spectrum of indole (Lautié et al., 1980; Harada & Takeuchi, 1986), can be assigned to exchange of the NH in the indole ring. MADH from strain W3A1 exhibits analogous RR spectral shifts in D_2O, particularly for the intense mode at ∼1450 cm^{-1}. This frequency undergoes a D shift of −6 cm^{-1} in MADH and −8 cm^{-1} in 6,7-IIQ (Table 1) and, thus, is likely to have significant NH bending character. In contrast, the RR spectra of MADHs from *T. versutus* and *P. denitrificans* and the 1450-cm^{-1} mode, in particular, are essentially unchanged by incubation in D_2O (Backes et al., 1991). Apparently, the NH of the tryptophylquinone cofactor in MADH from *T. versutus* or *P. denitrificans* is less accessible to solvent and simply not exchanging with deuterium.

No such deuterium dependence is observed for the ν(C═O) mode at 1638 cm^{-1} in 6,7-IIQ (Figure 3C) and 6,7-MIQ (data not shown). Since the large frequency shifts of ν(C═O) in polar solvents (Δaq in Table 1) indicate that the carbonyl oxygens are hydrogen bonded, we conclude that the hydrogen-bond strength is similar for H_2O and D_2O.

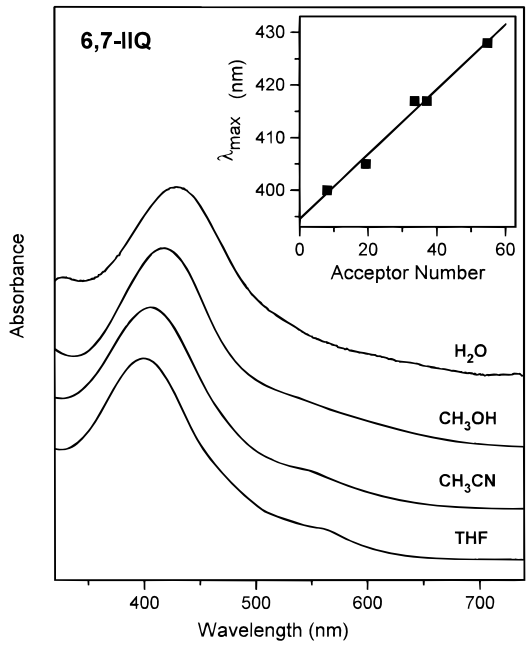

FIGURE 4: Absorption spectra of 6,7-IIQ ($\sim 10^{-4}$ M) in water and pure organic solvents. The aqueous sample was obtained by preparing a concentrated solution in DMSO and diluting it 100-fold in water. The inset shows a plot of the absorption maximum versus increasing solvent acceptor number for THF, CH_3CN, 2-propanol, CH_3OH, and H_2O.

Likewise, the C═O stretch in MADHs from *T. versutus* and *P. denitrificans* is insensitive to deuterium substitution (Backes et al., 1991) even though both carbonyl oxygens are H (or D) bonded to protein groups in the crystal structure (Chen et al., 1991).

Effect of Solvent Polarity on Indole Quinones. The addition of H_2O to acetonitrile solutions of 6,7-IIQ and 6,7-MIQ causes the ν(C═O) mode at 1650 cm^{-1} to decrease by 9−13 cm^{-1} and the δ(N−H) mode at 1461 cm^{-1} to decrease by 9 cm^{-1} (Table 1). These decreases were ascribed above to the electrostatic effects of hydrogen bonding of the carbonyl oxygen and NH proton of the indole quinone with water molecules. A more quantitative estimate of solvent influence has been achieved by investigating the effects of a series of organic solvents of different polarity and correlating spectral behavior with solvent acceptor number (Gutmann, 1978). First of all, the absorption spectrum of 6,7-IIQ is surprisingly sensitive to solvent polarity. The absorption maximum varies from 400 nm in the relatively nonpolar THF solvent to 425 nm in H_2O (Figure 4). The inset to Figure 4 shows a linear increase in λ_{max} with increasing acceptor number (i.e., with increasing hydrogen bonding ability). Second, the C═O stretch in the RR spectrum of 6,7-IIQ shows a similar dependence on solvent acceptor number, moving linearly to lower frequency with increasing hydrogen bonding ability of the solvent. As a result, there is a strong correlation between the ν(C═O) and λ_{max} of 6,7-IIQ (Figure 5, ■), such that higher values for λ_{max} and lower values for ν(C═O) are observed with increasing solvent polarity. The TTQ cofactor of MADH fits perfectly into this correlation (Figure 5, ●). Thus, the combined λ_{max} value of 440 nm and ν(C═O) value of 1612 cm^{-1} indicate that the hydrogen-bonding interactions between TTQ and the protein matrix in MADH are stronger than those between the indole quinone and water in 6,7-IIQ.

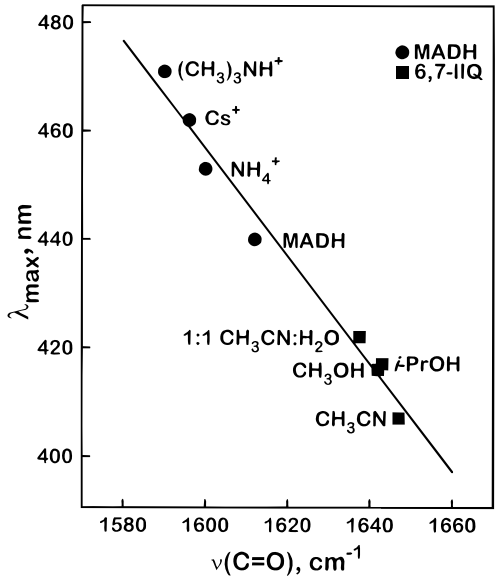

FIGURE 5: Correlation of the absorption maximum with the C═O stretching frequency for 6,7-IIQ (■) and MADH (●) in a series of different electrostatic environments. RR spectra and samples for 6,7-IIQ (Figure 2), for MADH (Figure 6), for Cs^+ and $(CH_3)_3NH^+$ adducts (Figure 7) and for NH_4^+ adduct (similar to Figure 7 but with 1 M NH_4Cl).

Effect of Cations on the TTQ Cofactor. $MADH_{ox}$ has been shown to interact with monovalent cations (Kuusk & McIntire, 1994; Gorren & Duine, 1994). The absorption maximum of *T. versutus* MADH is red-shifted from 440 nm in the absence of added cations to 453 nm with NH_4^+, 462 nm with Cs^+, and 471 nm with the inhibitory trimethylamine, $(CH_3)_3NH^+$ (Gorren et al., 1995a). Rapid scan experiments have detected a similar red-shifted intermediate during the enzymatic reaction of *T. versutus* MADH with the substrate, $CH_3NH_3^+$ (Gorren et al., 1995a).

The resonance Raman spectrum of *T. versutus* MADH is also sensitive to the presence of monovalent cations, exhibiting significant decreases in the C═O stretching frequency. Thus, the ν(C═O) at 1612 cm^{-1} in $MADH_{ox}$ (Figure 6) downshifts to 1596 (−16) cm^{-1} with Cs^+ and to 1590 (−22) cm^{-1} with $(CH_3)_3NH^+$ (Figure 7A,C). Although these ν(C═O) modes are weak spectral features, they are definitively identified by their disappearance from the ^{18}O-exchanged samples (Figure 7B,D). Difference spectra for the data in Figure 7 reveal that $\nu(C{=}^{18}O)$ has shifted underneath the 1580 cm^{-1} feature in both cases (data not shown). MADH from *P. denitrificans* has a more prominent ν(C═O) feature, and its −26 cm^{-1} shift upon addition of $(CH_3)_3NH^+$ (Table 1) is readily apparent in the raw data. As with 6,7-IIQ in different solvents, a number of other vibrational modes show small frequency shifts on cation binding. However, for both the MADH proteins and the indole quinone models, the C═O stretch at 1612−1639 cm^{-1} is by far the most strongly affected feature in the RR spectrum (Table 1). Furthermore, no RR spectral changes are observed upon addition of 1 M NaCl (data not shown), indicating that the observed effects are cation- rather than ionic-strength-dependent. Taken together, our RR results provide strong evidence that Cs^+ and $(CH_3)_3NH^+$ are interacting directly with a carbonyl oxygen of the TTQ cofactor.

The measured λ_{max} and ν(C═O) of $MADH_{ox}$ in the presence of cations have been included in Figure 5. They

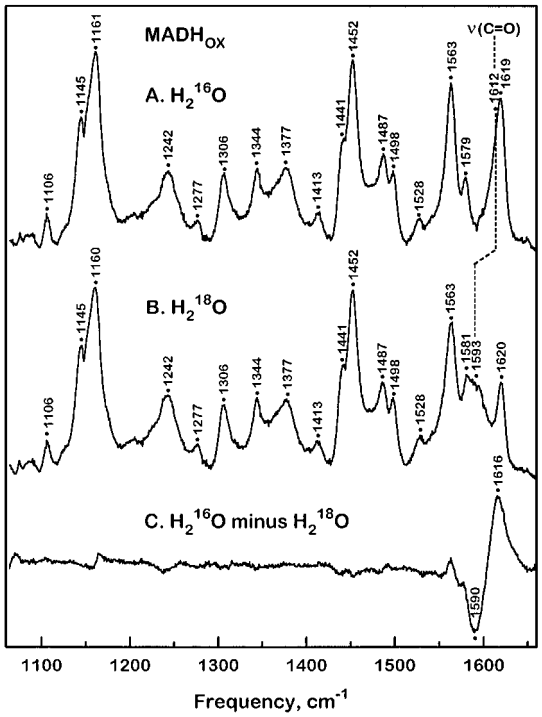

FIGURE 6: RR spectra of $MADH_{OX}$. Protein from *T. versutus* (0.2 mM) in 20 mM HEPES (pH 7.0). (A) Sample in $H_2{}^{16}O$. (B) Sample in $H_2{}^{18}O$. (C) Difference spectrum of A minus B. Spectra obtained with 488-nm excitation (10 mW) at 278 K.

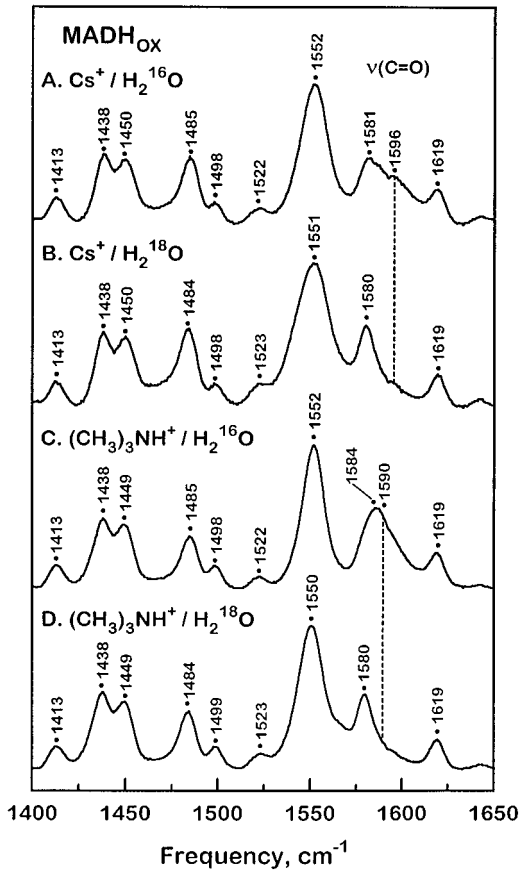

FIGURE 7: RR spectra of $MADH_{OX}$ with added cations. Sample and spectral conditions as in Figure 6. Samples contain (A) 500 mM CsCl in $H_2{}^{16}O$, (B) 500 mM CsCl in $H_2{}^{18}O$, (C) 10 mM $(CH_3)_3NHCl$ in $H_2{}^{16}O$, and (D) 10 mM $(CH_3)_3NHCl$ in $H_2{}^{18}O$.

show an excellent fit with the previous correlation for indole quinones, suggesting that the environment of the C═O groups of the TTQ cofactor increases in polarity in the order $NH_4^+ < Cs^+ < (CH_3)_3NH^+$. The strength of the interaction of these cations with the carbonyl group of TTQ follows the same order as their strength of binding to MADH: K_d values are 20 mM for NH_4^+, 4 mM for Cs^+, and 0.3 mM for $(CH_3)_3NH^+$ (Gorren & Duine, 1994; Gorren et al., 1995a). In the X-ray structure of *T. versutus* MADH, extra electron density was observed close to the oxygen of the C6 carbonyl group and was assigned to a water molecule or an ammonium ion from the crystallization medium (Huizinga et al., 1992). Our results favor the NH_4^+ assignment and provide strong evidence that other cations such as Cs^+ and $(CH_3)_3NH^+$ as well as the substrate, $CH_3NH_3^+$, occupy this same binding pocket adjacent to the C6 carbonyl of TTQ.

Effect of Cations on the MADH Semiquinone. Amicyanin carries out the reoxidation of $MADH_{red}$ *in vivo* in two one-electron steps, leading first to the formation of $MADH_{SQ}$ and then to $MADH_{ox}$ (Davidson, 1993). The first reoxidation step, $MADH_{red} \rightarrow MADH_{SQ}$, is strongly stimulated by the presence of monovalent cations, particularly NH_4^+ and Cs^+ (Kenny & McIntire, 1983; Gorren et al., 1995b). Addition of these cations to $MADH_{SQ}$ causes small shifts of 2−5 nm in the position of the absorption maximum and a broadening of line widths in the EPR spectrum (Kenny & McIntire, 1983; Gorren et al., 1995b). These changes led Gorren et al. (1995b) to propose a cation binding site and an electrostatic interaction with the semiquinone form of the cofactor. The increased rate of oxidation of $MADH_{red}$ was ascribed to stabilization of the SQ product by cations. We have now obtained additional evidence in support of this hypothesis from the effect of cations on the RR spectrum of $MADH_{SQ}$.

$MADH_{SQ}$ was produced by dithionite reduction of $MADH_{ox}$. The RR spectrum of the SQ is dominated by peaks at 1458 and 1527 cm^{-1} (Backes et al., 1991), with small peaks at 1565 and 1618 cm^{-1} being due to residual $MADH_{ox}$ (Figure 8A). To identify vibrational modes sensitive to the C-O group, we recorded RR spectra of the ^{18}O-semiquinone prepared from ^{18}O-$MADH_{ox}$ (with ^{18}O in the C6 position). Small downshifts of 1−2 cm^{-1} are observed for the peaks at 1458 and 1527 cm^{-1} as well as for several other peaks in the high frequency region (Figure 8A), but nothing as marked as the 23 cm^{-1} downshift for ν(C═O) in $MADH_{ox}$. This indicates that there is no pure C−O stretching mode in the RR spectrum of $MADH_{SQ}$. This is due, in part, to the decreased bond order of the C−O moiety which lowers the energy of the C−O stretch, allowing it to couple with other ring vibrations. However, the minimal ^{18}O-dependence also implies that the C6 carbonyl group of the cofactor is only weakly conjugated with the π system in the semiquinone state.

Addition of NH_4^+ to $MADH_{SQ}$ causes very little spectral change (Figure 8B), and the ^{18}O-exchanged $MADH_{SQ}$ exhibits similar ^{18}O-shifts (−1 cm^{-1} at 1388, 1459, and 1529 cm^{-1}) in the presence of NH_4^+ (Figure 8B) as in the absence of NH_4^+ (Figure 8A). This proves that the C6 oxygen is still present in the cofactor and has not been displaced by reaction with NH_4^+. Nevertheless, NH_4^+ does cause small spectral perturbations (relative to no adduct) at 1343 (−1), 1388 (+1), 1459 (+1), and 1529 (+2) cm^{-1}, and new peak intensity at 1479 cm^{-1}. The Cs^+ adduct of $MADH_{SQ}$ causes similar small perturbations (relative to no adduct) in the peaks at 1460 (+2) cm^{-1} and 1525 (−2) cm^{-1} (data not shown). Since these changes are generally beyond the experimental

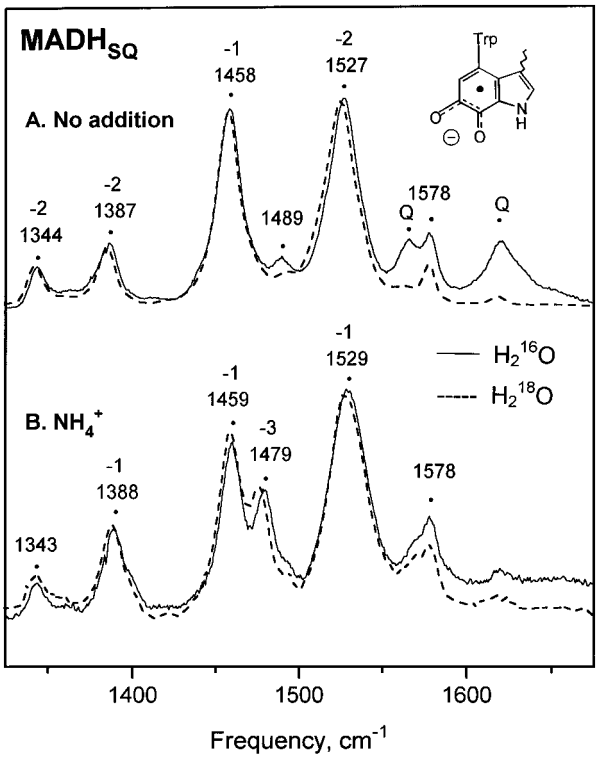

FIGURE 8: Effect of ^{18}O-substitution on the RR spectrum of $MADH_{SQ}$ in the presence and absence of ammonium ion. (A) In 25 mM Bicine (pH 9.0) in $H_2{}^{16}O$ (—) or $H_2{}^{18}O$ (- - -). (B) In 25 mM Bicine, 1 M NH_4Cl (pH 9.0) in $H_2{}^{16}O$ (—) or $H_2{}^{18}O$ (- - -). Spectra obtained with 442 nm excitation (10 mW) at 278 K. Peak frequencies are for $H_2{}^{16}O$ with $H_2{}^{18}O$ shifts indicated above. "Q" refers to peaks from residual $MADH_{OX}$ (formed by disproportionation of $MADH_{SQ}$).

error of ± 0.5 cm^{-1}, they indicate that the cations have altered the electrostatic environment of the cofactor. In addition, our data confirm the findings of Gorren et al. (1995b) that cations favor the formation of $MADH_{SQ}$. Both NH_4^+ and Cs^+ cause the disappearance of RR spectral contributions from $MADH_{ox}$ (Q in Figure 8A), most likely due to their favoring the comproportionation reaction: $MADH_{ox} + MADH_{red} \rightarrow 2MADH_{SQ}$.

In the enzymatic reduction of $MADH_{ox}$ by methylamine, the reduced form of the cofactor is an aminophenol. Subsequent reoxidation by amicyanin leads to an aminosemiquinone where the presence of the amino substituent has been verified by ESEEM spectroscopy and kinetics (Warncke et al., 1993; Bishop & Davidson, 1995). We have attempted to obtain RR spectroscopic evidence for an aminosemiquinone derived from methylamine reduction using two different procedures for preparing $MADH_{SQ}$: (i) by comproportionation of 1:1 mixture of oxidized and methylamine-reduced MADH, which yields a 1:1 mixture of O-SQ and N-SQ (Davidson et al., 1990), and (ii) by using cocrystallized MADH and amicyanin (Chen et al., 1992), whereby addition of methylamine causes reduction to the aminophenol and reoxidation by amicyanin yields a stable semiquinone (J. Sanders-Loehr, F. S. Mathews, and G. L. Rossi, unpublished results). Using either procedure, the RR spectrum of the resulting $MADH_{SQ}$ was identical to the O-form, and no spectral shifts were observed when the reaction was performed with [^{15}N]methylamine (data not shown). In the case of the TPQ cofactor of amine oxidase, the presence of an aminosemiquinone intermediate was readily identified by ^{15}N-isotope shifts of 3−4 cm^{-1} in the RR spectrum (Moënne-Loccoz et al., 1995). However, studies of MADH have indicated that the aminosemiquinone may be unstable at high protein concentrations (Warncke et al., 1993). Our failure to find any evidence for N-SQ in MADH suggests that the amino group was lost by hydrolysis before we were able to obtain a RR spectrum.

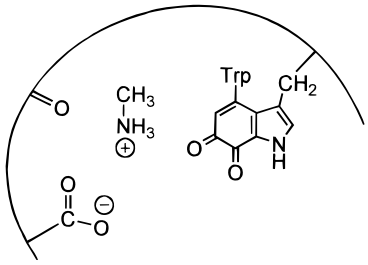

FIGURE 9: Proposed binding site for methylammonium substrate in MADH. The structure is based on X-ray data of Huizinga et al. (1992) and our finding that cationic competitive inhibitors interact with a carbonyl group of the TTQ cofactor.

CONCLUSIONS

The X-ray structure of $MADH_{ox}$ shows that the C6 carbonyl of the tryptophylquinone cofactor faces what appears to be the substrate-binding pocket and that the C6 carbonyl is the site of attack by nucleophilic suicide inhibitors (Chen et al., 1991; Huizinga et al., 1992). There is also electron density from an immobilized water or cation in close proximity to the oxygen of the C6 carbonyl carbonyl group (Huizinga et al., 1992). Further evidence for such a cation binding site comes from the fact that cations such as Cs^+, Rb^+, Li^+, and NH_4^+ as well as the substrate analogs $(CH_3)_2NH_2^+$, $(CH_3)_3NH^+$, and $(CH_3)_4N^+$ all behave as competitive inhibitors of the $CH_3NH_3^+$ substrate and all cause similar red-shifts in the absorption spectrum of the TTQ cofactor (Davidson & Jones, 1992; Kuusk & McIntire, 1994; Gorren & Duine, 1994). Furthermore, there is a strong correlation between K_d values obtained from kinetic inhibition studies and optical titrations, indicating that both measurements are probing the same cation binding site (Gorren & Duine, 1994). Our Raman experiments on ^{18}O-exchanged MADH show that these cations are not displacing the oxygen at the C6 position and, thus, are not reacting covalently with MADH. Cations such as Cs^+ and $(CH_3)_3NH^+$ do, however, cause the C═O stretching vibration of TTQ to downshift by 16−22 cm^{-1}. Comparison with model compounds shows that this type of downshift is exactly what is expected for a more polar environment in the vicinity of one or both of the carbonyl groups. Thus, our RR results provide the first direct evidence that monovalent cations are interacting with a carbonyl oxygen of the TTQ cofactor.

Since these cations behave as competitive inhibitors of methylamine oxidation, it is likely that the ammonium group of the substrate also binds in this location adjacent to the C6 carbonyl (Figure 9). In fact, a transient red-shift in the absorption spectrum has been observed upon addition of substrate (Gorren et al., 1995a), supporting the proposal that the first step in the enzymatic reaction is the electrostatic binding of $CH_3NH_3^+$ (Kuusk & McIntire, 1994; Gorren & Duine, 1994). According to the crystal structure, the cation binding site includes three additional carbonyl groups (peptide oxygens of residues 32, 104, and 106) and the side chain of Asp 32 and/or Asp 76 (Huizinga et al., 1992). A similar

binding site for monovalent cations has been identified in the crystal structure of rhodanese, where NH_4^+ or Cs^+ is coordinated to four peptide carbonyl oxygens and an aspartate side chain carboxylate (Kooystra et al., 1988). In MADH, alignment of the $CH_3NH_3^+$ substrate in the cation binding site (Figure 9) presumably favors proton abstraction from the amino group by one of the aspartate carboxylates. This arrangement would facilitate the nucleophilic attack by the substrate amine onto the C6 carbonyl of TTQ, the first step in the catalytic reaction.

The cations NH_4^+ and Cs^+, but not $(CH_3)_3NH^+$, have a different effect in the reductive half of the reaction cycle where they behave as activators in the amicyanin-catalyzed oxidation of $MADH_{red}$ to $MADH_{sq}$ (Gorren et al., 1995b). Interaction of these cations with the semiquinone form of the enzyme causes subtle changes in EPR line width and absorption maxima (Gorren et al., 1995b) as well as RR vibrational frequencies (present work), all of which are indicative of a direct electrostatic interaction of the cation with the cofactor. However, conformational changes due to cation binding at a longer distance from the active site have been observed in other systems (Peracchi et al., 1995) and cannot be ruled out in the present case. It is possible that the NH_4^+ reaction product is the physiological occupant of this cation binding site during the reductive half of the enzymatic reaction. If this binding reaction is utilizing the C6 oxygen of TTQ, then the ammonium ion would have to be displaced by substrate to start a new reaction cycle.

ACKNOWLEDGMENT

We are grateful to Drs. Victor L. Davidson, John McCracken, and F. Scott Mathews for helpful discussions.

REFERENCES

Backes, G., Davidson, V. L., Huitema, F., Duine, J. A., & Sanders-Loehr, J. (1991) *Biochemistry 30*, 9201−9210.

Bishop, G. R., & Davidson, V. L. (1995) *Biochemistry 34*, 12082−12086.

Carey, P. R. (1982) *Biochemical Applications of Raman and Resonance Raman Spectroscopies*, Academic Press, New York.

Chen, L., Mathews, F. S., Davidson, V. L., Huizinga, E. G., Vellieux, F. M. D., Duine, J. A., & Hol, W. G. J. (1991) *FEBS Lett. 287*, 163−166.

Chen, L., Durley, R., Poliks, B. J., Hamada, K., Chen, Z., Mathews, F. S., Davidson, V. L., Satow, Y., Huizinga, E., Vellieux, F. M. D., & Hol, W. G. J. (1992) *Biochemistry 31*, 4959−4964.

Davidson, V. L. (1993) in *Principles and Applications of Quinoproteins* (Davidson, V. L., Ed.) pp 73−95, Marcel Dekker, New York.

Davidson, V. L., & Jones, L. H. (1992) *Biochim. Biophys. Acta 1121*, 104−110.

Davidson, V. L., Jones, L. H., & Kumar, M. A. (1990) *Biochemistry 29*, 10786−10791.

Dooley, D. M., & Brown, D. E. (1993) in *Principles and Applications of Quinoproteins* (Davidson, V. L., Ed.) pp 275−305, Marcel Dekker, New York.

Duine, J. A. (1993) in *Microbial Growth on C_1 Compounds* (Murrell, J. C., & Kelly, D. P., Eds.) pp 401−413, Intercept Ltd., Andover, MD.

Gorren, A. C. F., & Duine, J. A. (1994) *Biochemistry 33*, 12202−12209.

Gorren, A. C. F., de Vries, S., Moënne-Loccoz, P., Backes, G., Sanders-Loehr, J., & Duine, J. A. (1995a) *Biochemistry 34*, 12926−12931.

Gorren, A. C .F., de Vries, S., & Duine, J. A. (1995b) *Biochemistry 34*, 9748−9754.

Gutmann, V. (1978) *The Donor-Acceptor Approach to Molecular Interactions*, Plenum, New York.

Harada, I., & Takeuchi, H. (1986) in *Spectroscopy of Biological Systems* (Clark, R. J. H., & Hester, R. E., Eds.) pp 113−175, John Wiley, New York.

Huizinga, E. G., van Zanten, B. A. M., Duine, J. A., Jongejan, J. A., Huitema, F., Wilson, K. S., & Hol, W. G. J. (1992) *Biochemistry 31*, 9789−9795.

Itoh, S., Ogino, M., Komatsu, M., & Ohshiro, Y. (1992) *J. Am. Chem. Soc. 114*, 7294−7295.

Itoh, S., Ogino, M., Haranou, S., Terasaka, T., Ando, T., Komatsu, M., Ohshiro, Y., Fukuzumi, S., Kano, K., Takagi, K., & Ikeda, T. (1995) *J. Am. Chem. Soc. 117*, 1485−1493.

Kenney, W. C., & McIntire, W. (1983*) Biochemistry 22*, 3858−3868.

Kooystra, P. J. U., Kalk, K. H., & Hol, W. G. J. (1988) *Eur. J. Biochem. 177*, 345−349.

Kuusk, V., & McIntire, W. S. (1994*) J. Biol. Chem. 269*, 26136−26143.

Lautié, A., Lautié, M. F., Gruger, A., & Fakhri, S. A. (1980) *Spectrochim. Acta 36*, 85.

Loehr, T. M., & Sanders-Loehr, J. (1993) *Methods Enzymol. 226*, 431−470.

McIntire, W. S., Wemmer, D. E., Chistoserdov, A. E., & Lidstrom, M. E. (1991a) *Science 252*, 817−824.

McIntire, W. S., Bates, J. L., Brown, D. E., & Dooley, D. M. (1991b) *Biochemistry 30*, 125−133.

Moënne-Loccoz, P., Nakamura, N., Steinebach, V., Duine, J. A., Mure, M., Klinman, J. P., & Sanders-Loehr, J. (1995) *Biochemistry 34*, 7020−7026.

Nonaka, Y., Tsuboi, M., & Nakamoto, K. (1990) *J. Raman Spectrosc. 21*, 133−141.

Ohshiro, Y., & Itoh, S. (1994) *Pure Appl. Chem. 66*, 753−758.

Peracchi, A., Mozzarelli, A., & Rossi, G. L. (1995) *Biochemistry 34*, 9459−9465.

Singh, S. N., & Singh, R. S. (1968) *Spectrochim. Acta 24A*, 1591−1597.

van Wielink, J. E., Frank, J., & Duine, J. A. (1990) *Methods Enzymol. 188*, 235−241.

Warncke, K., Brooks, H. B., Babcock, G. T., Davidson, V. L., & McCracken, J. (1993) *J. Am. Chem. Soc. 115*, 6464−6465.

BI952641Q